Hindawi
International Journal of Chemical Engineering
Volume 2022, Article ID 4617664, 12 pages
https://doi.org/10.1155/2022/4617664

Research Article

Combined Effect of Compression Ratio and Fuel Injection Pressure on CI Engine Equipped with CRDi System Using *Prosopis juliflora* Methyl Ester/Diesel Blends

T. Ramesh[1], **A. P. Sathiyagnanam**[2], **Melvin Victor De Poures**[3] and **P. Murugan**[4]

[1]*Department of Mechanical Engineering, Annamalai University, Annamalainagar, Chidambaram 608002, Tamil Nadu, India*
[2]*Department of Mechanical Engineering, Government College of Engineering, Salem (Deputed from Annamalai University), Tamil Nadu, Salem 636011, India*
[3]*Department of Mechanical Engineering, Saveetha School of Engineering, SIMATS, Chennai- 602105, Tamil Nadu, India*
[4]*Department of Mechanical Engineering, Jimma Institute of Technology, Jimma University, Ethiopia*

Correspondence should be addressed to T. Ramesh; rameshthambaiyan69@gmail.com and A. P. Sathiyagnanam; apsgnanam@gmail.com

Received 8 March 2022; Revised 27 March 2022; Accepted 6 April 2022; Published 29 April 2022

Academic Editor: G.L. Balaji

The exhaustion of worldwide oil reserves has created an incipient need to find hopeful alternative fuels for the future. Substantial research has been done in this direction, and all studies by researchers have provided results that proved the growing potential of biofuel as a popular alternative in the CI engine. The current investigation explores the biofuel potential derived from the wasteland tree *Prosopis juliflora* (Karuvalam tree seeds). Experimentation was done using a monocylinder 4-stroke water-cooled six holes CRDi CI engine with electrical loading. The experiment was conducted at three proportions (10%, 20%, and 30% volume basis) of *Prosopis juliflora* Oil Methyl Ester (PJOME) with diesel using 3 parametric CRs (16, 17.5, and 19) along with three different fuel injection pressure (FIP) (400, 500, and 600 bar). The impact of CR and FIP on fuel utilization BTE, cylinder pressure, net heat release, and exhaust particulates was scrutinized and characterized. The test results demonstrated that increasing the compression ratio from 16 to 19 enhanced the in-cylinder pressure, net heat release (NHR), and BTE for all the (PJOME/Diesel) combinations. With an augmentation in the compression ratio from 16 to 19, carbon monoxide and unburnt hydrocarbon discharge diminished, but the nitrogen oxide discharges augmented. FIP also had an impact of increasing the pressures on the in-cylinder, NHR, brake thermal efficiency, and nitrogen oxide and reducing the emissions of smoke, CO, and UBHC. The current research shows that the use of B20 and CR16 and FIP 600 bar as a combination improved BTE by 33.21%, BSFC by 0.25 kg/kw-hr, cylinder pressure at the maximum to reach 69.28 bar, net heat release of 79.14 J/deg, and exhaust emissions such as UHC at 55 ppm, CO at 0.25%, smoke at 34.33%, and NOx at 2401 ppm. Finally, the BTE and NOx were slightly higher, and the UHC, CO, and smoke values were diminutive compared to other blends.

1. Introduction

The huge rise in vehicles, along with the rapid exhaustion of global oil sources, gave rise to a high requirement for crude contrivances. In recent decades, the globe's energy demand has been encouraging the world to look for new sources of energy [1]. A developing nation like India is interested in producing biodiesel from nonedible oils, which are widely cultivated in the country's wasteland [2]. The government regulates emission standards for greenhouse gases due to the problem of climate change and human health. Biodiesel usage has reduced CO, HC, and PM tailpipe discharges [3]. Biodiesel serves as a successful fuel substitute for diesel. Vegetable oil is a suitable replacement for diesel because it has similar qualities and it is renewable. Since the last century, investigators have examined the utilization of vegetable oils. Vegetable oils possess approximately a similar potential when utilized in diesel engines with somewhat less thermal efficiency. Reduced engine emissions are an important part of engine development research which focuses

increasingly on environmental protection and strict recirculation of exhaust gases [4]. The prominent biodiesel items currently regarded as substitutes for fuel are biodiesel, wasteland products such as *Jatropha*, Pongamia oil, *Prosopis juliflora* seed, rapeseed, and sunflower. These fuel sources are clean combustible, renewable, nontoxic, biologically degradable, and ecological, capable of being utilized as a clean variant or capable of being combined with diesel and petroleum. The *Prosopis juliflora* seed oil is relatively new and appears as the most suitable alternative for diesel fuel [5]. The results showed that the *Prosopis juliflora* is a nonpalatable material used for biodiesel generation in parched and partially parched areas. Solvent extraction technology from *Prosopis juliflora* has been employed for oil extraction. Free fatty acids in *Prosopis juliflora* oil were reduced, as measured by a drop in potassium hydroxide/gm from 43.7 mg to 8.6 mg/gm and then to 2.7 mg/gm during the two stages of the esterification process for biodiesel with 1 percent v/v of H_2SO_4 and a two-hour minimum reaction period. The characteristics of the refined biodiesel after the transesterification process, including CN, consistency, acid values, and calorific number, agreed with the ASTM standards [6]. The researchers exposed diesel engines as having a bad environmental effect since they contain large levels of sulfur and aromatic materials. CO, SOx, NOx, and smoke are formed from exhaust emissions from diesel fossil fuels [7]. It has been discovered that the performance of diesel engines operating on biodiesel mixtures is significantly affected by engine characteristics such as the injection timing and compression ratio. In order to address these difficulties, several creative technologies are developed to incorporate the changes in current engine designs [8]. It shows, currently, new ideas for improving engine development technologies and pollution control concepts are infrequently investigated. Results were examined to analyze the impact of the engine's physical characteristics like CR, FIP, and functionality characteristics like combustible depletion, thermal efficacy, and the regular undesirable discharges under the usage of JME. The system had a FIP of 240 bar, CR of 18, brake specific fuel consumption improvement by 10%, and brake thermal efficiency enhancement by 8.9%. In view of the increased emissions due to higher compression ratios, the emission of the HC and exhaust was increased, while the emission of smoke and CO was reduced [9]. The increased pressure of the fuel injections (FIP) causes the injected fuel droplets to decrease in size, which leads to improved atomization and quicker evaporation of fuel particles. The result will be more thorough fuel combustion, leading to better thermal efficiency and enhanced power generation. Furthermore, with the increased FIP, the combustion delay time was shortened. This reduces the mixture in a shorter time and significantly reduces the quantity of nitrogen oxide (NOx) produced by the period of inflammation. Dhinakaran et al. investigated the effects of ZJME mixed with diesel and aluminum nanoparticles on the CRDI CI system's combustion, functionality, and discharge parameters [10]. The inclusion of Al_2O_3 NPs in a biodiesel-diesel blend improved the BTE and heat release rate significantly [11]. The research reported the lemon peel oil (LPO) and orange peel oil (OPO) experiments in the CRDI engine. Three distinct characteristics analyses which included the dosage pressures, split addition, and EGR were done. At six hundred bar pressure and 10% pilot addition, the OPO outperformed the diesel along with LPO in terms of brake thermal efficiency [12]. et al. reiterated that substantial waste of fatty, high-quality fuel could be incurred. The 70% bioconstituent blends were preferred for CRDI engines, while the diesel performance of the engine can be assumed to be degraded slightly [13]. Karanja biodiesel tests were conducted on a CRDI diesel engine. The uncontrolled and controlled exhausts were examined at different engine paces (1500, 2000, and 3500 revolutions per minute) with B20 Karanja biodiesel mixture and diesel on behalf of different engine loading scenarios (0%, 20%, 40%, 80%, and 100% specified loading). CO and HC were only released under low engine loads. In comparison to diesel at top engine loads, the nitrogen oxide emissions were elevated in the B20. Solomon et al. investigated the functionality, incineration, and discharge physiognomies of a CRDI system by implementing a high bioethanol fraction in various types of biodiesel-diesel variants [14]. The biodiesel derived from animals and safflower-canola biodiesel were utilized. In lower and higher load situations, the animal-based biodiesel blends were more successful than the safflower-canola biodiesel blends in reducing hydrocarbon (HC) emissions, whereas the carbon monoxide (CO) emissions elevated with the rise in bioethanol concentration in both blends. At higher loads, higher bioethanol concentrations in blends can minimize the NOx emissions and smoke opacity. Turkcan et al. researched combustion, performance, and emission parameters under various engine loads driven by a linseed petroleum biodiesel and a diesel mixture. The engine was therefore powered at 2200 rpm motor speeds and various loads of engine by biodiesel blends (D100, L10, L20, and L30). With the L10 mix excluding 3.75 Nm and full loading conditions, the higher cylinder pressure was noticed [15]. Uyumaz et al. reported engine experiments which were carried out using a variable compression ratio using acetylene and diesel. Their findings revealed that the maximum pressure and the heat release rate grew by means of a greater compression ratio and TE [16]. Vijayaragavan et al. conducted studies on compression ratio, which elevated the CR, thereby augmenting the TE along with the nitrogen oxide discharges. As a result, it would be ideal if the difficulty of increased nitrogen oxide emissions at enhanced CR could be reduced, devoid of sacrificing engine performance [17]. The exhaust gas recirculation (EGR) approach is a well-known mechanism for reducing NOx emissions at the tailpipe [18]. The effect of various FI techniques (FIP and FIT) as well as a $C_4H_{10}O/C_{12}H_{23}$ mix (20% $CH_{10}O$-Bu20) was reported on system functionality and emissions. The investigational outcomes demonstrated an enhanced fuel injection pressure (100 MPa) and augmented incineration parameters over a reduced fuel injection pressure (65 MPa). The improved FIT in combination with the Bu20 blend improves combustion characteristics while lowering UBHC and CO emissions. At every FIP and FIT, the Bu00 had somewhat higher NOx emissions [19]. It is observed that soot nanoparticle

properties were altered by reducing the number (by an average of 7) and size (by an average of 5) of primary particles, which resulted in decreased PM concentrations [20]. This work replicated the influences of FI settings on incineration, functionality, discharge parameters, and particle rudiments. At 3 fuel injection pressures (400, 700, and 1000 bar) and 4 SoMI durations (4, 6, 8, and 10 deg bTDC), biodiesel variants B20 (20% v/v biodiesel and 80% v/v diesel) and B40 (40% v/v biodiesel and 60% v/v diesel) were correlated to the threshold reserve fuel. The particulate morphology of biodiesel exhaust revealed decreased main constituents in granulated groupings, leading to lower malignancy and ecologically conducive [21].

According to the literature, while some investigations were conducted to appraise the eminence of injection timing (IT) and FIP on the system functionality parameters of a diesel engine functioning with various biodiesel/diesel combinations, the CRDi systems operating using biodiesel (PJOME) variants were not investigated. The influence of CR and FIP, as well as a fraction of *Prosopis juliflora* Oil Methyl Ester concentration invariants, on the incineration, functionality, and discharge parameters of a monocylinder CRDi aided diesel engine was not investigated in the expositions. The literature clearly shows that this subject requires additional investigation to fill a research gap. The current research aims to investigate the effects of CR and FIP on the functionality, incineration, and discharge parameters of a CRDi diesel engine running on PJOME/Diesel mix in an experimental setting.

1.1. Novelty of the Work. The novel aspects of the current study are summarized: (i) the fuel obtained from *Prosopis juliflora* oil can be used as a novel feedstock; (ii) modifications in variable compression ratio (CR) and fuel injection pressure (FIP) were made to the engine to get the best possible engine performance and emissions reduction.

2. Research Methodology

2.1. Prosopis juliflora Oil (PJO). Prosopis *juliflora* is a dicotyledon in the Fabaceae family and the Mimosoideae subfamily. *Prosopis juliflora* is a robust species that offers fuelwood and forage to India's parched and partially parched regions. These trees are capable of breeding in brackish places, natural alkali soils, seashore areas, desert sand dunes, Indian river ravines, and arid and damaged grasslands. The Fabaceae-based *Prosopis juliflora* tree can reach a height of 10m and a width of 15m, depending on the species. The wood of *Prosopis juliflora* is porous (spate irrigation system). The tree is covered with thorns, which may or may not be present in some branches. Figure 1 depicts a flowering and fruiting *Prosopis juliflora* tree (pods). *Prosopis juliflora* pods (fruit) appear almost flat. The pods have a length of 1 feet, a width of 5–15 mm, and a thickness of 3-9 mm. The mature pods become mushy and yellowish-brown, changing from green to yellowish-brown. Each inflorescence contains between 1 and 16 (pods) fruits. Seeds have a span of 6.5 mm and weight in a range of 0.20 and 0.32 g (20000–32000 seed/kilogram). Husks weighing 5 kg to 10 kg per tree can be produced premised on the weather scenarios and ecology. It is expected that *Prosopis juliflora* may produce 2230 kg/ha pods at a density of roughly 20 kg/tree (A technical manual on managing *Prosopis juliflora*). Figure 1 depicts a photograph of the *Prosopis juliflora* seeds and powder. The necessary extent of the PJ kernels could be collected from desolated areas throughout its recurrent time, and the kernels were refined by cleansing and then aerated in the sunshine to eliminate dampness. These aerated kernels are ground in order to segregate oil.

2.2. Transesterification. The unrefined oil segregated from the desiccated seed of the PJ has elevated viscosity and meagre incineration excellence as a result of fatty acids. The *Prosopis juliflora* oil sustained transesterification for minimizing the viscidity enabling flammability. The crude jojoba oil was inducted into the reactor in an estimated volume and subjected to heating in a slow manner till 65 °C. Subsequent to this, the combination of stimulant (CH_3NaO) and CH_3OH was inducted into the activator. The combination was mixed incessantly for 3 hours and the temperature was sustained at 65°C. During this time, the chemical response happens among unrefined jojoba oil and CH_3OH. When the response was concluded, the combination was sapped and conveyed to the disconnecting channel. The stage segregation happened in the channel in two deposits. Biodiesel occupied the top zone, and the bottom zone was occupied by glycerine. In the end, the rinsing was done with H_2O. Figure 2 demonstrates the transesterification process.

2.3. Preparation of Prosopis juliflora Methyl Esters and Their Properties. The transesterified oil is mixed with diesel in weight percentages of 10%, 20%, and 30%, referred to as B10, B20, and B30, accordingly. To determine the stable blend, multiple quantities of diesel and biooil were tried. It was discovered that blends containing 10% PJOME and 90% diesel by volume, 20% PJOME and 80% diesel by volume, and 30% PJOME and 70% normal diesel by volume are largely balanced and consistent for an extended period of time. The dynamics were investigated in order to determine its potential as a fuel for CI engines. All the blends' combustible characteristics, such as compactness, flash point, viscosity, and substantial assessment, are taken into account. In Table 1, a few characteristics of biooil and diesel can be noticed. The biodiesel was combined with 10% petrodiesel, and the parameters were compared to petrodiesel. The biodiesel was then blended with 20% and 30% neat diesel. A similar methodology of discriminating the characteristics and estimating the identical features was repeated. At the same time, the 10% combination was comparable to petrodiesel.

2.4. Gas Chromatograph-Mass Spectrometer Analysis. The *Prosopis juliflora* methyl ester (B100) is analyzed using gas chromatography spectrography to determine the chemical components present. The chromatographic spectrums of PJOME are depicted in Figure 3. The chromatogram displays numerous chemicals with different retention

Figure 1: *Prosopis juliflora* pods, seed powder, and *Prosopis juliflora* oil.

(a) (b)

Figure 2: Picture of (a) soxhlet reactor apparatus and (b) transesterification setup.

Table 1: Properties of test fuels.

Property	Standard	Diesel	B10%	B20%	B30%	PJOME
Density (kg/m^3)	ASTM *D* 1298	813	832	839	847	886
Kinematic viscosity @40 °C (cst)	ASTM *D* 445	2.42	2.63	2.81	3.04	4.64
Calorific value (MJ/kg)	ASTM *D* 240	42.5	42.23	41.95	41.6	39.025
Flash point (°C)	ASTM *D* 93	58	69.4	74	81	118
Fire point (°C)	ASTM *D* 93	67	77	82	93	130
CCI	ASTM *D* 976	47	49.6	55.3	58.2	41.76

times. The GC-MS data reveals the presence of nitriles, aromatic amines, alkenes, and alkanes. The primary fatty acids are lauric acid, myristic acid, and palmitic acid, along with minor ingredients. This shows that *Prosopis juliflora* methyl ester is mostly saturated fatty acids. Table 2 lists the components and their retention times.

2.5. Engine Test Rig and Procedure. The experimental setup is depicted in Figure 4. A Kirloskar diesel engine with a specified power yield of 3.5 kW at 1500 rpm was utilized in the experiment. The engine was a monocylinder, 4-stroke, CRDI water-cooled type with a dynamometer. The CRDI was provided with appropriate receptors and drivers to facilitate electronic feed along with an open electronic control unit that met Nira i7r specs. A CRDI arrangement was required to achieve the insertion pressures needed for the evaluation. The fuel delivery line was changed to accommodate the engine's CRDI arrangement, and an elevated pressure pump was included subsequent to the fuel filter. This balustrade is connected to the common rail and functions as a combustible reserve, allowing it to be kept at

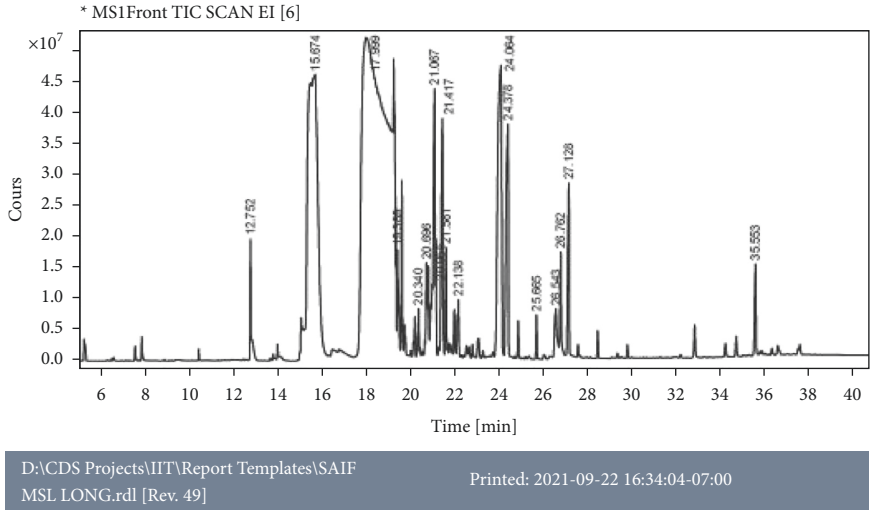

Figure 3: GC-MS analysis of *Prosopis juliflora* oil.

Table 2: GC-MS analysis composition of *Prosopis juliflora* oil.

Fatty acids	Formula	Systematic name	Retention time
Lauric acid	C12H24O2	Dodecanoic acid (C12)	21.48
Myristic acid	C14H28O2	Tetradecanoic acid (C14)	26.76
Palmitic acid	C16H32O2	Hexadecanoic acid (C16)	15.68
Stearic acid	C18H38O2	Octadecanoic acid (C18)	18.00
Oleic acid	C18H34O2	Cis-9- octadecanoic acid (C18 : 1)	26.54
Linoleic acid	C18H32O2	Cis-9-cis12-octadecanoicacid (C18 : 2)	22.14
Arachidonic acid	C20H40O2	Eicosanoic acid (C20)	27.13
Behenic acid	C22H44O2	Docosenoic acid (C22)	24.06

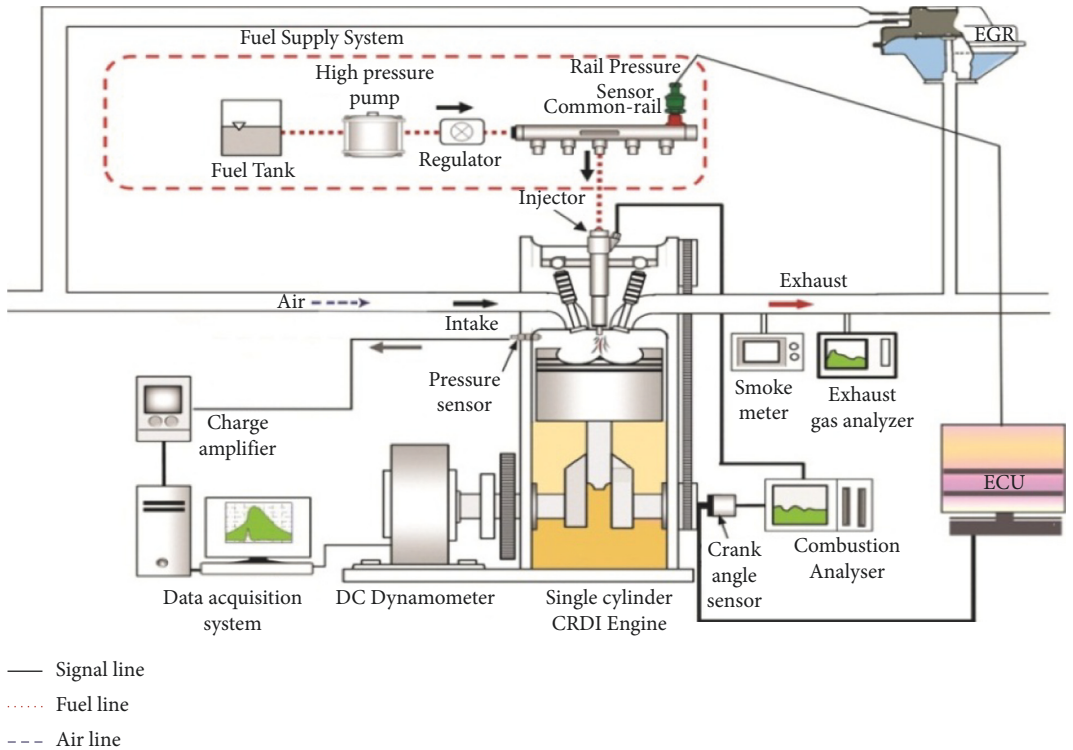

Figure 4: Layout of the experimental setup.

the insertion pressure. For sustaining the combustible pressure, a rail pressure detector is installed on the railing and subsequently connected to the Nira i7r ECU. A 6-hole solenoid-organized feeder was chosen to undertake this task because the previous injector is not capable of managing the significantly higher feed pressures that will be functional using CRDI. After setup, the ECU is used to map the new sensors and actuators, and the configuration is changed to make sure that all the workings are working properly. If the system functions properly, it is considered ready for testing. The benefits of a multicylinder engine aligning CRDI technology-enhanced feed pressures and different administration approaches deserved the implantation of CRDI for the test in monocylinder employment. Exhaust smoke emissions are estimated using the AVL 437C smoke meter, and nitrogen oxide discharges are measured using the AVL digas 444N exhaust emissions appraiser. Table 2 lists the test engine's technical details. A photographic picture of the engine test setup is revealed in Figure 5. Test engine technical particulates are shown in Table 3.

In these proposed examinations, studies were conducted on the CRDI with assistance from a diesel engine. For every trial, the functionality evaluation was performed at the specified pace of 1500 rpm. Three test fuels (B/*D* blends) were used in the evaluations, which were identified as B10, B20, and B30. The experiments were carried out using the mentioned fuels by altering the CR (16, 17.5, and 19) and the FIP (400 bar, 500 bar, and 600 bar). The instrument ranges and accuracy are shown in Table 4.

2.6. Error Analysis. The equipment calibration or measurement results can be affected by a variety of factors, including the environment, test preparation, and reading. The uncertainty analysis is necessary to establish the accuracy of the experiments [22]. This section computes the faults connected with different instruments along with parameter estimations. Moffat (1985) provided a correlation for evaluating the highest probable error in calculation. The least evaluation of the fewest characteristics along with the equipment accurateness was evaluated for errors. If a standard total S is dependent on independent parameters such as (X_1, X_2, X_3... X_n), then the condition is used to determine the mistakes in S estimations by using

$$\left(\frac{\partial s}{s}\right) = \left\{\left(\frac{\partial X_1}{X_1}\right)^2 + \left(\frac{\partial X_2}{X_2}\right)^2 + \ldots\ldots + \left(\frac{\partial X_n}{X_n}\right)^2\right\}^{1/2}, \quad (1)$$

where $(\partial X_1/X_1)$, $(\partial X_2/X_2)$ are the mistakes in the self-sufficient parameters. X_1 represents the measuring instrument's minimum accuracy and ∂X_1 characterizes the least rate estimated from the investigations. Equation (2) can be used to indicate inaccuracies in the calculation of brake thermal efficiency (BTE) because it is derived from fuel consumption [23].

Figure 5: Test engine photographic view.

Table 3: Test engine technical particulates.

Make and Model	Kirloskar, TV1
Number of cylinders	One
Stroke	Four
Bore	87.5 mm
Stroke length	110 mm
Swept volume	661 cc
Compression ratio	17.5
Rated output	3.5 kW at 1500 rpm
Rated speed	1500 rpm
Cooling system	Water-cooled
Injection timing, CA bTDC	23°
Injection pressure	600 bar

Table 4: Range, accuracy, and resolution of the instruments.

Quantity	Range	Accuracy	Resolution
AVL smoke meter	0–100%	±1%	0.1%
AVL gas analyzer	NOx: 0–5000 ppm	±5 ppm	1 ppm vol
	HC: 0–30000 ppm	±10 ppm	1 ppm vol
	CO: 0–15%	±0.02%	0.01%vol
	CO_2: 0–20%	±0.3%	0.01%vol
Engine speed	400. . .6000 min^{-1}	±1 min^{-1}	1 min^{-1}
Oil temperature	0–125 °C	±4°C	1°C

$$\left(\frac{\partial BTE}{BSFC}\right) = \left\{\left(\frac{\partial \text{torque}}{\text{torque}}\right)^2 + \left(\frac{\partial rpm}{rpm}\right)^2 + \left(\frac{\partial \text{time}}{\text{time}}\right)^2\right\}^{1/2}. \quad (2)$$

From equation (2), the maximum error calculation of BTE and BSFC is around 0.41%. Likewise, the errors related to the measure of temperature, cylinder pressure, and crank angle were determined to be 0.53%, 1.35%, and 2.18%, respectively.

3. Outcomes and Analysis

Investigations were done in 2 stages in the current study. In the preliminary stage, the CR was varied, and in the secondary stage, the fuel injection pressure was changed. The impact of changing the 2 characteristics on the CRDI system assisted the diesel engine's combustion, performance, and exhaust parameters when using the four evaluation fuels that

were analyzed. The experimental results for the rated load situation are discussed in the subsequent sections.

3.1. Performance Analysis of PJOME/Diesel Mixtures

3.1.1. Brake Thermal Efficiency (BTE). Figure 6 portrays the impact of compression ratio and FIP on the BTE of the three different test fuels. When the compression ratio is varied from 16 to 19, the brake thermal efficiency gets augmented for all the 3 evaluation combustibles. This occurs because as CR rises, more combustibles are fed at an enhanced pressure and temperature, facilitating enhanced fuel-air combination and faster combustible evaporation [24]. As a result, at higher CR, the BTE is greater. The brake thermal efficiency for the 3 different evaluation combustibles exists as a result of FIP implementation. The highest BTE for a B20 fuel occurs at 600 bar at full load condition. Increased FIP results in a reduction in the combustible globule dimension during the fuel injection. This resulted in increased fuel evaporation and enhanced combination with the peripheral air. This increases the burning efficacy and the brake thermal efficiency [25]. The varied CR and FIP rates indicate that B20 blends have a higher BTE value than other test fuels such as B10 and B30. In comparison to the other two test fuels, the combination of B20 blends, CR 16, and FIP 600 bar produces the greatest BTE of 33.2%. The main reason for this is that high FIP fuel droplets are split into small particles that can be injected into a cylinder faster than in typical low FIP systems. In addition, the sprayed fuel is thoroughly blended with compressed air. To achieve more rated power, retard the CR value when the FIP is high, which could be due to the fact that more negative work does not have to be done on the piston if the maximum pressure is reached before the TDC [9].

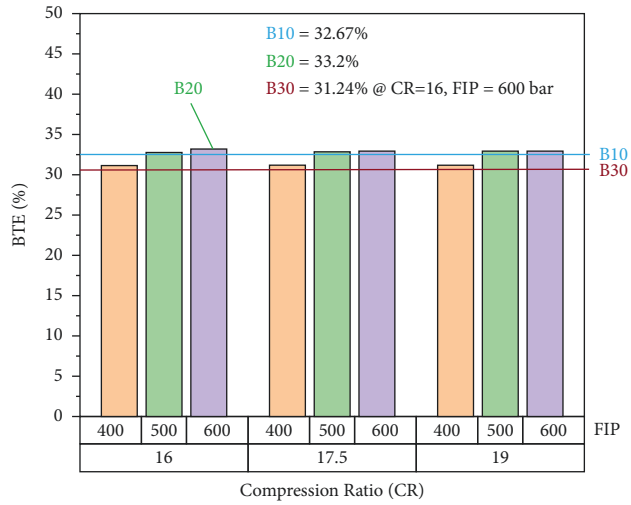

Figure 6: BTE for B20 blend at various FIP and CR.

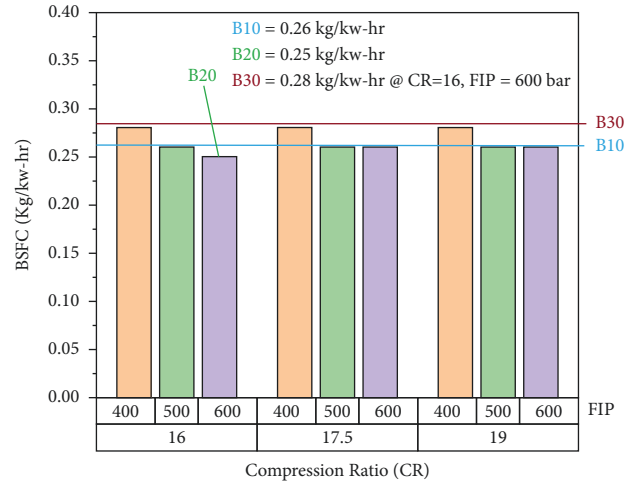

Figure 7: BSFC for B20 blend at various FIP and CR.

3.1.2. Brake Specific Fuel Consumption (BSFC). Figure 7 demonstrates the CR's influence and the FIP on the BSFC of three different test fuels. Figure 7 illustrates the specific fuel consumption of various fuels. On full load, the B10 mixtures consumed 0.26 kg/kWh of a specific fuel. The SFC increases mostly as the concentration of PJOME increases. As a result, B20 and B30 blends produced 7.6% less SFC than B10 at an increase in CR and FIP. BSFC is dependent on the density and gross calorific number of biodiesel. When the density of biodiesel falls, BSFC content decreases as well. Biodiesel generates less power with the same amount of fuel due to its lower gross calorific value [26]. For the CR 16 and FIP 600 bar, B20 had the best BSFC at full loads when compared to the blends like B10 and B30. In comparison to the other test mixtures, the combination of B20 mixes, CR 16, and FIP 600 bar operations results in lower specific fuel consumption of 0.25 kg/kWh.

3.2. Emission Analysis of PJOME/Diesel Mixtures

3.2.1. Unburned Hydrocarbon (UHC). Figure 8 reveals the hydrocarbon emissions for a variety of FIP and CR configurations. Increased CR and FIP rates reduce the unburned emissions in most cases. All of the test fuels saw significant drops in UBHC emissions. At increasing CRs, the air and combustion temperatures rise, which induces this phenomenon [26]. When fuel injection pressure rises, the unburnt hydrocarbon discharges fall and attain a low followed by a subsequent rise. The crucial appraisal of the fuel injection pressure at which the minimum unburned hydrocarbon emissions occur was determined to be 600 bar for the B20 variant at CR16. UBHC emissions are reduced due to better combustion and smaller combustible droplets when the FIP is increased. However, as the fuel injection pressure is elevated more, the droplets' dimension reduces, and the velocity increases. It leads to an increase in UBHC emissions because of the combustible globules impacting the cylinder barriers [27]. The HC emission (ppm) was noted for a CR of 16, FIP of 600 bar, and 100% of the load. Sample B20 emitted the least HC at 55 ppm, while the blend B10 and B30 emitted HC at 58 ppm and 62 ppm, respectively, which is 6% and 12.7% higher than B20. It was revealed that, as the concentration of the PJ increases in the B20, the amount of emitted HC also increases.

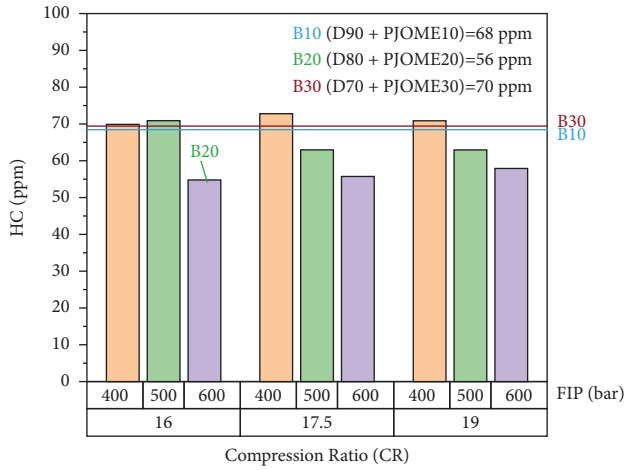

Figure 8: HC emission for B20 blend at different FIPs and CRs.

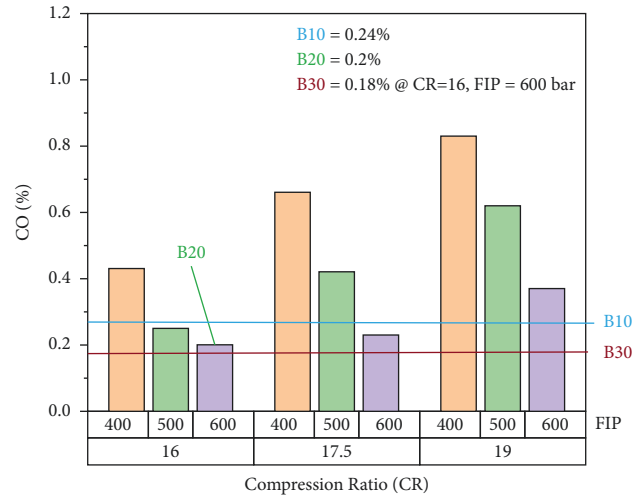

Figure 9: CO emission for HX20 blend at different FIPs and CRs.

3.2.2. Carbon Monoxide (CO). Figure 9 shows the carbon monoxide emissions for B10%, B20%, and B30% PJOME mixes at various CRs and FIPs. Figure 9 shows that for all of the test fuels, the CO emissions rise as the CR rises from 16 to 19. The B20 and B30 blends produce less CO_2 than the PJOME's B10 blends at any CR, according to the research. This is due to the PJOME's chemical structure having higher oxygen content. The CO emissions are reduced when biofuel is used in engines [28]. According to Figure 10, the CO emissions decrease as the FIP increases from 400 to 600 bar for B20 and B30 blends, but the CO emissions increase beyond these FIP values. As previously stated, a greater FIP results in smaller combustible constituents and enhances air-fuel blending, which enables improved combustion. As a result, the CO emissions are reduced [27]. As per the final results, the B20 and B30 mixtures at CR16 and FIP 600 bar emit the least amount of CO when compared to the B10 mixture. The B20 and B30 variants have carbon monoxide discharge values of 0.2% and 0.18% (vol), accordingly.

3.2.3. Oxide of Nitrogen (NOx). Figure 10 depicts the effect of CR and FIPs on NOx emissions. According to Figure 10, as the CR increases from 16 to 19, the nitrogen oxide discharges are enhanced for all the 3 evaluation combustibles. The nitrogen oxide emissions elevate by 5.39%, 3.2%, and 6.28% for B10, B20, and B30 mixtures, respectively. The CR has been raised from 16 to 19. The amount of NOx produced is mostly determined by the combustion temperature. As previously stated, a greater CR leads to a higher combustion temperature and, as a result, leads to higher NOx generation [28]. Due to a rise in FIP, NOx emissions increased. The amount of oxygen present in the incineration cubicle throughout the incineration procedure, as well as the in-cylinder gas temperature, has a major impact on NOx generation [29]. Finally, the optimum results of B20 (CR of 16 and FIP of 600 bar) emit 2401 ppm of NOx at full load, which is lower than the other biodiesel blends.

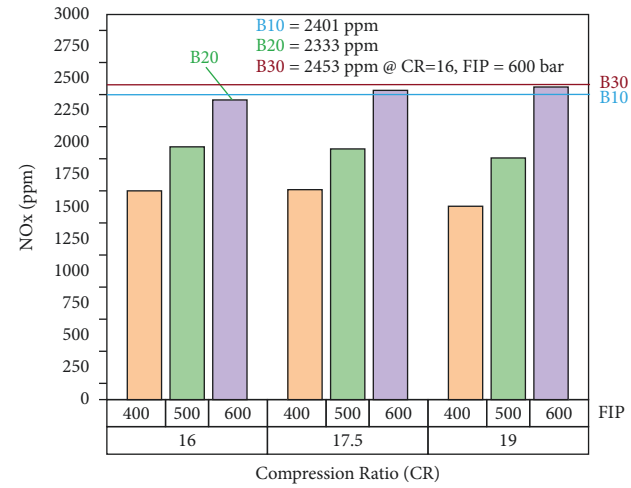

Figure 10: NOx emission for B20 blend at various FIPs and CRs.

3.2.4. Smoke Opacity (SO). The incomplete fuel combustion aids in the production of smoke, aiding the smoke opacity. Figure 11 shows an unexpected presence of smoke elements in the effluvium. It is stated unequivocally that smoke generation rises with increasing CR for all test fuels. The amount of smoke in the environment has been substantially reduced as the engine FIPs increased [30].

Secondly, higher biodiesel in fuel blends lowered the smoke emissions. When fully loaded, the B30 reduced smoke emissions by 18.91% on average versus the B10 at CR16. The oxygen content of the biodiesel and full combustion result in lower smoke production with fuel blends when compared to B10. It has been shown that an increase in FIP reduces smoke emissions significantly. An ideal fuel injection pressure exists further than which the smog discharge increases proportionately with the fuel injection pressure. 600 bar were found as the optimal pressure for the B20 blends. First, an augmentation in fuel injection pressure leads to elevated fuel perforation and a mixture of air fuel inside the combustion chamber. This produces cleaner combustion and

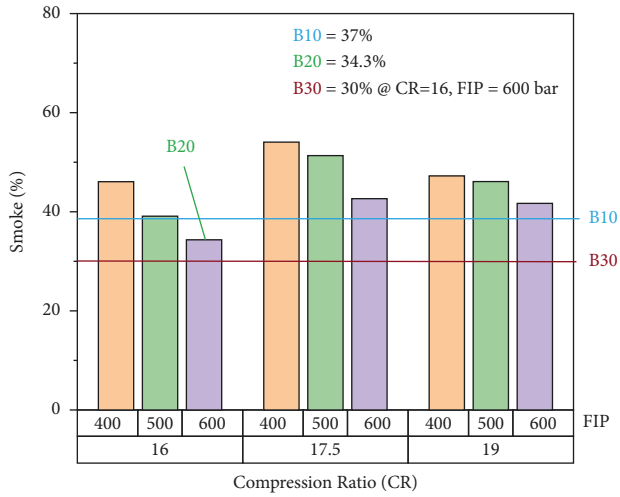

Figure 11: Smoke opacity for B20 blend at various FIPs and CRs.

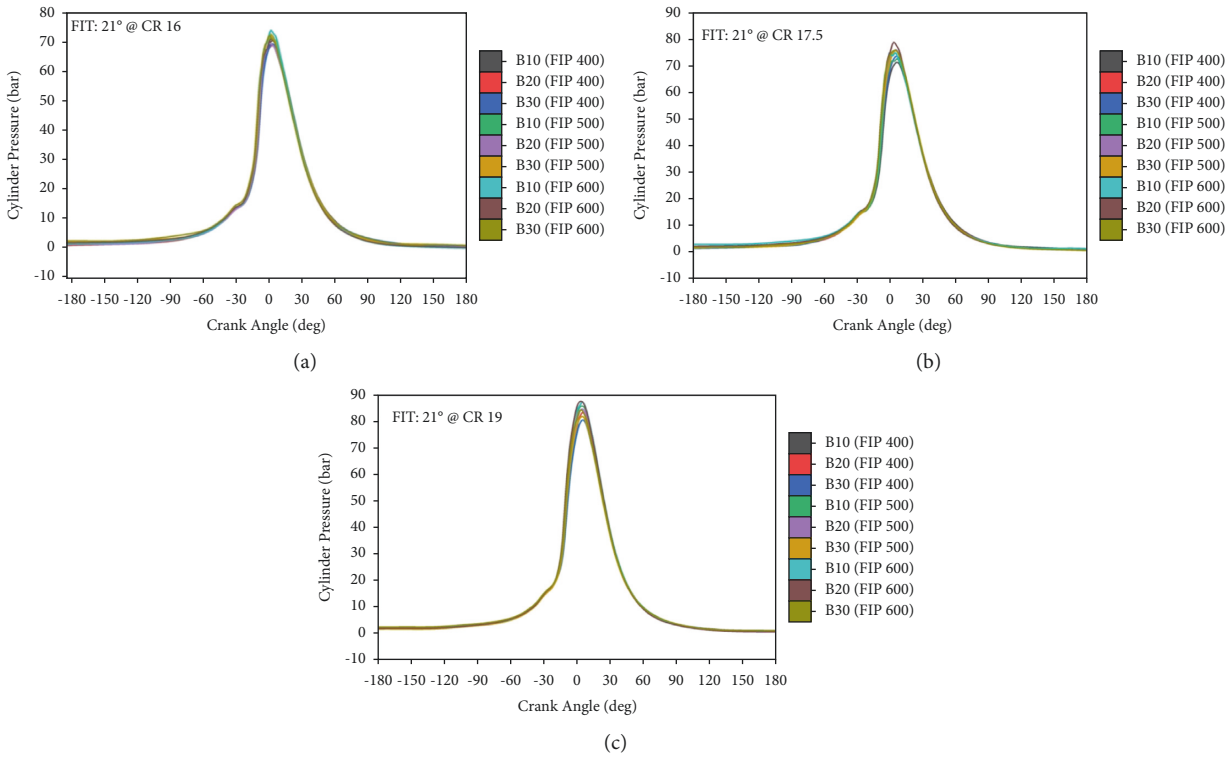

Figure 12: (a) Crank angle vs cylinder pressure at CR 16 and different FIPs. (b) Crank angle vs cylinder pressure at CR 17.5 and different FIPs. (c) Crank angle vs cylinder pressure at CR 19 and different FIPs.

lowers the smoke emissions [21]. The smoke opacity of B20 at CR16, and FIP 600 bar, was lower than that of the other two test fuels, as seen in the graph.

3.3. Combustion Analysis of PJOME/Diesel Mixtures. The performance and emission parameters clearly indicate that the B20 blend of *Prosopis juliflora* Oil Methyl Ester (PJOME) is the best test fuel mixture in the mentioned engine trial conditions. So, the combustion parameter analysis is done for the optimal blend B20 for verification.

3.3.1. Cylinder Peak Pressure (CPP). The incineration process of an IC configuration is elucidated by the inside gas pressure when it is operated. The pressure statistic is equated to above 150 sequences to reduce the influence of the sequence to sequence variation. Figures 12(a)–12(c) estimate the fluctuations in pressure vs crank angle for all the evaluation combustibles at CRs of 16, 17.5, and 19 and FIP of 400, 500, and 600 bar. The effect may be demonstrated using Figure 12, which shows how the increase of CR from 16 to 19 increases the peak pressure. The statistics reveal that the combustion center is closer to TDC as a result of the

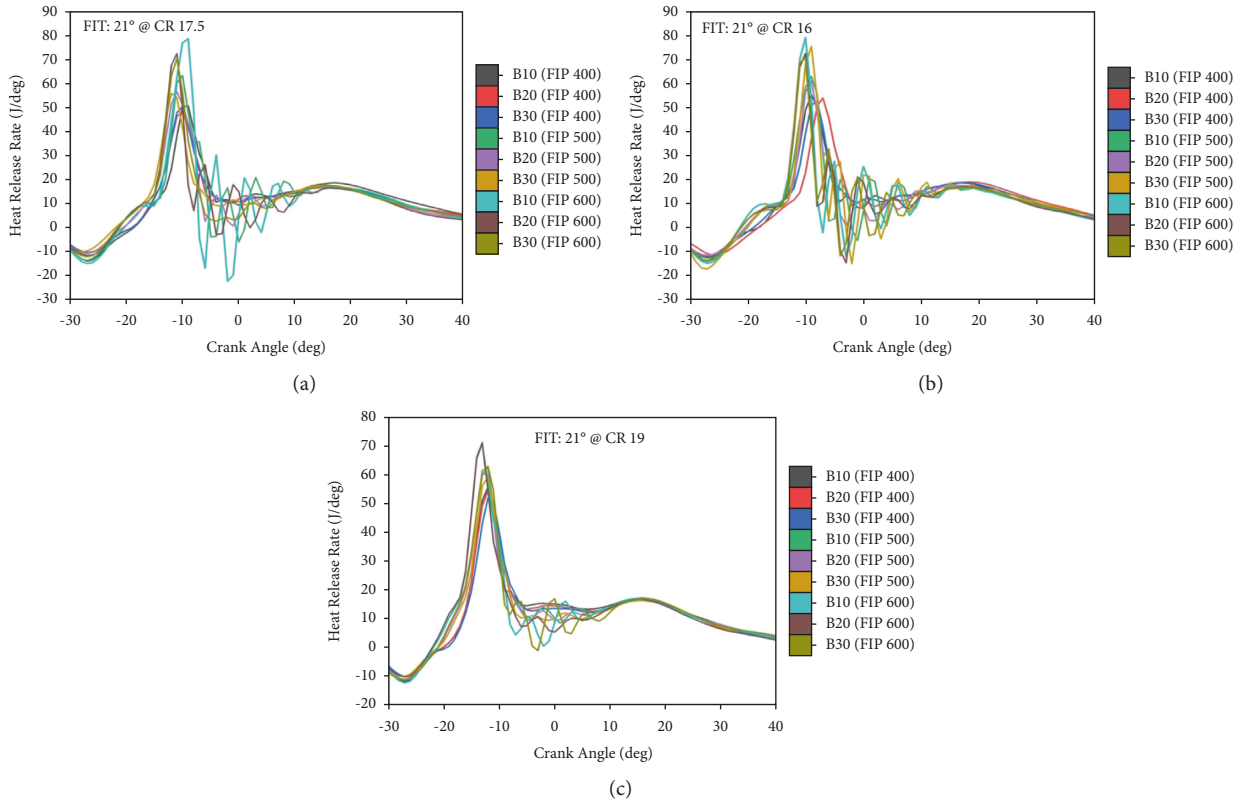

Figure 13: (a) Crank angle vs cylinder pressure at CR 16 and different FIPs. (b) Crank angle vs cylinder pressure at CR 17.5 and different FIPs. (c) Crank angle vs cylinder pressure at CR 19 and different FIPs.

precursory feed of the evaluation combustibles, which raises the peak pressure [19].

The highest peak pressure values were found for B20 at CR of 16 and a FIP of 600 bar. The blend B20 possessed a peak pressure of 69.28 bar, whereas the blends B30 and B10 had values of 69.2 and 66.55 bar, respectively. An uncontrolled combustion stage and oxygen percentage availability in biodiesel resulted in the highest peak pressures. This can be attributed to its reduced CN, elevated self-ignition temperature, and elevated latent heat. All the mentioned reasons cause inflated pressure peaks from prime to later ignition [29]. Increasing the FIP values increases the ignition delay time, allowing more combustion events at TDC and a decrease in peak pressure [28].

3.3.2. Net Heat Release Rate (NHRR). Figures 13(a)and 13(c) show HRR against the crank angle for all the evaluator combustibles at 16, 17.5, and 19 compression ratios and 400, 500, and 600 bar FIP. The profiles of the HRR provide assessable facts on the progress of incineration. The heat release rate identifies the extent of synthetic vivacity emitted in combustion. The heat release rate is related to the cylinder pressure measurements. In a diesel engine, combustion involves precombined incineration and dispersion. The high oxygen concentration of the biodiesel blends resulted in a longer premixed combustion phase, as the oxygenates possess a reduced CN value, allowing increased fuel to build within the incineration enclave, resulting in quick flaming and enhanced heat release rate summits [27]. Among the B20 fuels tested, a greater premixed combustion stage was observed. This is due to the prevalence of oxygen in the test mixture. The physical delay can also be influenced by air temperature, pressure, turbulence, and velocity. The oxygen concentration can be adjusted to shorten the synthetic impediment duration.

The higher O_2 level in the B20 combination transpired in a greater heat release rate than the B10 and B30 mixes. Regardless of the compression ratio, the ignition delay will no longer be due to the lower evaporation rate of the fuel. If this happens, additional fuel may collect in the incineration cubicle, increasing the heat release rate after the incineration process has started, which was previously considered [28]. At FIP 600 bar, the maximum HRR for the B10, B20, and B30 blends at CR16 was 72.55 J/deg, 79.14 J/deg, and 70.43 J/deg, accordingly, at complete loading scenarios.

4. Conclusion

Experimental studies were done on a CRDi engine using PJOME/Diesel blends (10%, 20%, and 30% of PJOME-by volume) in order to evaluate the impact of CR and FIP on the combustion, performance, and emission parameters. 3 distinct evaluation combustibles were used, namely, 10%, 20%, and 30% PJOME blends. The CR was varied from 16 : 1 to 19 : 1, and the FIP was varied from 400 to 600 bar in increments of 100 bar. The testing was done at the rated load

at a constant speed. The experimental results revealed the following:

All three test fuels, increasing the CR and FIP, enhanced the top in-cylinder pressure, NHR, and brake thermal efficiency. B20 at a higher FIP of 600 bar and CR of 16 had the highest result, with a BTE of 33.2%.

The BSFC of all the three evaluation combustibles rises as the CR is increased from 16 to 19. When the FIP increased from 400 to 600 bar, the BSFC for B20 and B30 mixtures dropped by 7.14%.

With increments of CR and FIP, the NOx formation is greater for all the three evaluation combustibles. The NOx emissions climbed by 33.61% in the B10, 26.98% in B20, and 28.73% in B30 when the CR was increased from 16 to 19 and the FIP from 400 to 600 bar. The NOx particulates for the fraction blend, i.e., B20, were lower for any CR and FIP.

For all the three evaluation fuels, UHC emissions enhanced as the higher CR. UHC emissions increased by 14.71%, 5.17%, and 5.83% for the B10, B20, and B30 blends, accordingly, as the CR increased from 16 to 19. The UHC tendency, on the other side, reverses up until the critical FIP. The UHC was reduced by 16.74%, 21%, and 11.29%, respectively, for B10, B20, and B30 blends, with a FIP rise from 400 to 600 bar. At any point, the B20 blend produced the lowest possible UHC emissions at CR16 and FIP 600 bar.

The CO emissions increased for all the evaluation fuels when the compression ratio was augmented. But in a vice versa manner, the CO emissions reduced as the FIP increased. The CR increased from 16 to 19, as the CO emissions increased by 22.07%, 25.43%, and 28%, respectively, and the FIP increased from 400 to 600 bar. For the B10, B20, and B30 blends, the CO emissions decreased by 44.06%, 30.93%, and 28.92%, respectively. At CR of 16 and FIP of 600 bar, the CO emissions were optimum for the B20 blend.

When the compression ratio was changed from CR 16 to 19 and FIP from 400 to 600 bar, the smoke opacity was reduced. The FIP of 600 bar and CR of 16 reduced the smoke output by 19.48% and 17.54%, respectively, when compared to the CR of 17.5.

4.1. Future Research Prospects. In this investigation, the B20 (PJOME20) blend performed exceptionally well when compared to other blends. In spite of this, the blend's NOx discharges were enhanced compared to pure diesel operation. Future investigations on the implementation of the combination in CI engine applications should keep the following issues in mind:

Further investigation is required to find the influence of EGR on different engine parameters

Advanced sustainability assessment tools, such as exergoeconomic and exergoenvironmental assessments, could be used to conduct a sustainability study

It is possible to investigate the congruity of the Cetane boosters in the binary blend [31]

Data Availability

The data used to support the findings of this study are included within the article. Should further data or information be required, these are available from the corresponding author upon request.

Conflicts of Interest

The authors declare that there are no conflicts of interest regarding the publication of this paper.

Authors' Contributions

T. Ramesh participated in writing the original draft, reviewing and editing the manuscript, and conceptualization. A. P. Sathiyagnanam contributed to the investigation and supervision. Melvin Victor De Poures did the resources. P. Murugan made project administration.

Acknowledgments

The authors thank Annamalai University, Annamalainagar, for providing characterization support to complete this research work.

References

[1] M. Mikulski, K. Duda, and S. Wierzbicki, "Performance and emissions of a CRDI diesel engine fuelled with swine lard methyl esters–diesel mixture," *Fuel*, vol. 164, pp. 206–219, 2016.

[2] D. N. Basavarajappa, N. R. Banapurmath, S. V. Khandal, and G. Manavendra, "Performance evaluation of common rail direct injection (CRDI) engine fuelled with Uppage Oil Methyl Ester (UOME)," *International Journal of Renewable Energy Development*, vol. 4, no. 1, pp. 1–10, 2015.

[3] S. P. Venkatesan, S. Ganesan, J. J. Prabhahar, V. R. Kaveti, A. Anoop, and A. Andrew, "Performance and emission test on diesel engine using *Prosopis juliflora* seed oil," *International Journal of Ambient Energy*, vol. 32, pp. 1–6, 2020.

[4] V. Karthickeyan, B. Dhinesh, and P. Balamurugan, "Effect of compression ratio on combustion, performance and emission characteristics of DI diesel engine with orange oil methyl ester," in *Bioresource Utilization and Bioprocess*, S. K. Ghosh, R. Sen, H. N. Chanakya, and A. Pariatamby, Eds., pp. 131–149, Springer, Berlin, Germany, 2020.

[5] G. S. G. Selvan, "Experimental analysis of VCR engine operated with *Prosopis juliflora* biodiesel blends," *International Journal of Renewable Energy Resources*, vol. 2, pp. 980–987, 2020.

[6] M. Rajeshwaran, P. Ganeshan, and K. Raja, "Optimization and biodiesel production from Prosopis julifera oil with high free fatty acids," *Journal of Applied Fluid Mechanics*, vol. 11, no. 1, pp. 257–270, 2018.

[7] M. A. Asokan, S. Senthur Prabu, P. K. K. Bade, V. M. Nekkanti, and S. S. G. Gutta, "Performance, combustion and emission characteristics of juliflora biodiesel fuelled DI diesel engine," *Energy*, vol. 173, pp. 883–892, 2019.

[8] S. Yogeshwaran, L. Natrayan, S. Rajaraman, S. Parthasarathi, and S. Nestro, "Experimental investigation on mechanical properties of Epoxy/graphene/fish scale and fermented spinach hybrid bio composite by hand lay-up technique," *Materials Today Proceedings*, vol. 37, no. 2, pp. 1578–1583, 2021.

[9] K. Siva Prasad, S. Srinivasa Rao, and V. R. K. Raju, "Effect of compression ratio and fuel injection pressure on the characteristics of a CI engine operating with butanol/diesel blends," *Alexandria Engineering Journal*, vol. 60, no. 1, pp. 1183–1197, 2021.

[10] D. Veeman, M. S. Sai, P. Sureshkumar, T. Jagadeesha, L. Natrayan, and M. Ravichandran, "Additive manufacturing of biopolymers for tissue engineering and regenerative medicine: an overview, potential applications, advancements, and trends," *International Journal of Polymer Science*, vol. 2021, Article ID 4907027, 20 pages, 2021.

[11] C. S. Aalam, C. G. Saravanan, and M. Kannan, "Experimental investigations on a CRDI system assisted diesel engine fuelled with aluminium oxide nanoparticles blended biodiesel," *Alexandria Engineering Journal*, vol. 54, no. 3, pp. 351–358, 2015.

[12] B. Ashok, K. Nanthagopal, D. Arumuga Perumal, J. M. Babu, A. Tiwari, and A. Sharma, "An investigation on CRDi engine characteristic using renewable orange-peel oil," *Energy Conversion and Management*, vol. 180, pp. 1026–1038, 2019.

[13] V. Shahir, C. Jawahar, V. Vinod, and V. Vinod, "Experimental investigation on performance and emission characteristics of a common rail direct InjectionEngine using animal fat biodiesel blends," *Energy Procedia*, vol. 117, pp. 283–290, 2017.

[14] L. N, L. Y. Solomon Jenoris Muthiya, "Mohankumar subramaniam, joshuva arockia dhanraj, wubishet degife mammo, "development of active CO_2 emission control for diesel engine exhaust using amine-based adsorption and absorption technique," *Adsorption Science and Technology*, vol. 2022, Article ID 8803585, 8 pages, 2022.

[15] A. Turkcan, "Effects of high bioethanol proportion in the biodiesel-diesel blends in a CRDI engine," *Fuel*, vol. 223, pp. 53–62, 2018.

[16] A. Uyumaz, "Experimental evaluation of linseed oil biodiesel/diesel fuel blends on combustion, performance and emission characteristics in a DI diesel engine," *Fuel*, vol. 267, Article ID 117150, 2020.

[17] M. Vijayaragavan, B. Subramanian, S. Sudhakar, and L. Natrayan, "Effect of induction on exhaust gas recirculation and hydrogen gas in compression ignition engine with simarouba oil in dual fuel mode," *International Journal of Hydrogen Energy*, vol. 47, pp. 1–13, 2021.

[18] R. Shanmugam, D. Dillikannan, G. Kaliyaperumal, M. V. De Poures, and R. K. Babu, "A comprehensive study on the effects of 1-decanol, compression ratio and exhaust gas recirculation on diesel engine characteristics powered with low density polyethylene oil," *Energy Sources, Part A: Recovery, Utilization, and Environmental Effects*, vol. 43, no. 23, pp. 3064–3081, 2021.

[19] M. A. Fayad, "Effect of renewable fuel and injection strategies on combustion characteristics and gaseous emissions in diesel engines," *Energy Sources, Part A: Recovery, Utilization, and Environmental Effects*, vol. 42, no. 4, pp. 460–470, 2020.

[20] M. A. Fayad, H. A. AL-Salihi, H. A. Dhahad, F. M. Mohammed, and B. R. AL-Ogidi, "Effect of post-injection and alternative fuels on combustion, emissions and soot nanoparticles characteristics in a common-rail direct injection diesel engine," *Energy Sources, Part A: Recovery, Utilization, and Environmental Effects*, vol. 34, pp. 1–15, 2021.

[21] A. P. Singh and A. K. Agarwal, "Evaluation of fuel injection strategies for biodiesel-fueled CRDI engine development and particulate studies," *Journal of Energy Resources Technology*, vol. 140, no. 10, 2018.

[22] H. A. Dhahad, M. A. Fayad, M. T. Chaichan, and T. Megaritis, "Influence of fuel injection timing strategies on performance, combustion, emissions and particulate matter characteristics fueled with rapeseed methyl ester in modern diesel engine," *Fuel*, vol. 306, Article ID 121589, 2021.

[23] P. Asha, L. Natrayan, B. T. Geetha et al., "IoT enabled environmental toxicology for air pollution monitoring using AI techniques," *Environmental Research*, vol. 205, Article ID 112574, 2022.

[24] V. K. Shahir, C. P. Jawahar, V. Vinod, and P. R. Suresh, "Experimental investigations on the performance and emission characteristics of a common rail direct injection engine using tyre pyrolytic biofuel," *Journal of King Saud University - Engineering Sciences*, vol. 32, no. 1, pp. 78–84, 2020.

[25] C. S. Aalam, C. G. Saravanan, and B. P. Anand, "Impact of high fuel injection pressure on the characteristics of CRDI diesel engine powered by mahua methyl ester blend," *Applied Thermal Engineering*, vol. 106, pp. 702–711, 2016.

[26] P. Kanthasamy, V. A. M. Selvan, and P. Shanmugam, "Investigation on the performance, emissions and combustion characteristics of CRDI engine fueled with tallow methyl ester biodiesel blends with exhaust gas recirculation," *Journal of Thermal Analysis and Calorimetry*, vol. 141, no. 6, pp. 2325–2333, 2020.

[27] L. Natrayan, V. Sivaprakash, and M. S. Santhosh, "Mechanical, microstructure and wear behavior of the material AA6061 reinforced SiC with different leaf ashes using advanced stir casting method," *International Journal of Engineering and Advanced Technology*, vol. 8, pp. 366–371, 2018.

[28] Q. Li, F. Backes, and G. Wachtmeister, "Application of canola oil operation in a diesel engine with common rail system," *Fuel*, vol. 159, pp. 141–149, 2015.

[29] D. Damodharan, A. P. Sathiyagnanam, D. Rana, B. Rajesh Kumar, and S. Saravanan, "Extraction and characterization of waste plastic oil (WPO) with the effect of n -butanol addition on the performance and emissions of a DI diesel engine fueled with WPO/diesel blends," *Energy Conversion and Management*, vol. 131, pp. 117–126, 2017.

[30] T. Sathish, K. Palani, L. Natrayan, A. Merneedi, M. V. De Poures, and D. K. Singaravelu, "Synthesis and characterization of polypropylene/ramie fiber with hemp fiber and coir fiber natural biopolymer composite for biomedical application," *International Journal of Polymer Science*, vol. 2021, Article ID 2462873, 8 pages, 2021.

[31] M. A. Fayad and H. A. Dhahad, "Effects of adding aluminum oxide nanoparticles to butanol-diesel blends on performance, particulate matter, and emission characteristics of diesel engine," *Fuel*, vol. 286, Article ID 119363, 2021.